Influence of strain on the anti-ferromagnetic ordering in epitaxial Cr(001) films on MgO

E Kunnen, S. Mangin, V Moshchalkov, Y Bruynseraede, A Vantomme, A. Hoser, K Temst

ELSEVIER

Thin Solid Films 414 (2002) 262–269

thin solid films

www.elsevier.com/locate/tsf

Influence of strain on the anti-ferromagnetic ordering in epitaxial Cr(001) films on MgO

E. Kunnen[a], S. Mangin[a], V.V. Moshchalkov[a], Y. Bruynseraede[a], A. Vantomme[b], A. Hoser[c], K. Temst[a,*]

[a]*Laboratorium voor Vaste-Stoffysica en Magnetisme, Katholieke Univ. Leuven, Celestijnenlaan 200 D, B-3001 Leuven, Belgium*
[b]*Instituut voor Kern—en Stralingsfysica, K.U. Leuven, Celestijnenlaan 200 D, B-3001 Leuven, Belgium*
[c]*Hahn-Meitner-Institut, Glienicker Strasse 100, D-14109 Berlin, Germany*

Received 4 January 2001; received in revised form 7 March 2002; accepted 13 March 2002

Abstract

The influence of epitaxial strain on the anti-ferromagnetic ordering was studied in a 450-nm-thick Cr film grown on a MgO(001) substrate by molecular beam epitaxy. The anti-ferromagnetic nature of the films was probed by neutron diffraction. A detailed structural characterization of the film was carried out by atomic force microscopy, Rutherford backscattering/channeling spectrometry, and X-ray diffraction. At low temperatures a transverse spin density wave with propagation vector in the film plane is detected, and is attributed to the presence of epitaxial strain. Crystal defects in the sample lead to the appearance of the commensurate anti-ferromagnetic state at higher temperatures.

Keywords: Chromium; Epitaxy; Magnetic structures; X-Ray diffraction; Rutherford backscattering spectroscopy; Neutron scattering

1. Introduction

During the last decade the interest in the intrinsic magnetic properties of thin Cr films has increased strongly. This was partly motivated by the intensive studies carried out on Fe/Cr superlattices, one of the archetypal multilayer systems in which the giant magneto-resistance (GMR) effect has been encountered [1]. Various physical aspects of the constituent materials and their interfaces have been studied in detail. It was established, for instance, that the interface roughness in Fe/Cr superlattices has a profound influence on the magnitude of the GMR effect [2,3]. The role of the anti-ferromagnetic ordering in the Cr spacer layers has been another major issue in the understanding of the observed oscillatory exchange coupling effects. In order to clarify this point, several studies have focused on the intrinsic magnetic properties of *thin Cr films* embedded in a superlattice. Meersschaut et al. [4] used the perturbed angular correlation technique (PAC) to study epitaxial Fe/Cr superlattices, grown by molecular beam epitaxy (MBE), and found that the anti-ferromagnetic ordering breaks down below a thickness of 6 nm, suggesting that anti-ferromagnetic ordering in Cr cannot play a dominating role in the oscillatory exchange coupling. Fullerton et al. [5] used transport and magnetization measurements to demonstrate that in sputtered, epitaxial Fe/Cr superlattices the anti-ferromagnetic order is suppressed for Cr layer thickness below 4 nm and that the anti-ferromagnetic ordering of the Cr layers significantly changes the interlayer coupling since the biquadratic coupling of the Fe layers was observed to disappear below the Néel temperature T_N of the Cr layers. Further direct information about the anti-ferromagnetic nature of Cr in Fe/Cr superlattices has been provided by neutron diffraction measurements, demanding experiments for which the sample requirements are very high. Fullerton et al. [6] and Schreyer et al. [7] investigated the commensurate and incommensurate anti-ferromagnetic phases in Cr layers embedded in an Fe/Cr superlattice. These diverse studies made clear that the

*Corresponding author. Tel.: +32-16-32-76-20; fax: +32-16-32-79-83.
E-mail address: kristiaan.temst@fys.kuleuven.ac.be (K. Temst).

0040-6090/02/$ - see front matter
PII: S0040-6090(02)00285-7

anti-ferromagnetic nature of the Cr films can be profoundly influenced by subtle variations in the crystalline order, strain in the film, proximity with paramagnetic or ferromagnetic layers, etc.

As a reference for the study of anti-ferromagnetic order in thin Cr films, a comparison can be made with the anti-ferromagnetic (AF) structure of *bulk single crystal Cr*, which is well known. The main properties are summarized in the review by Fawcett [8]. Below the onset of anti-ferromagnetism at the (bulk) Néel temperature $T_N = 311$ K, the spins are sinusoidally modulated along the [001] and equivalent axes, resulting in an incommensurate spin density wave (SDW) characterized by a wave vector **Q**. The period of this SDW is slightly temperature dependent and varies between 80 Å at room temperature and 60 Å at 4.2 K [9]. Above the spinflip temperature $T_{sf} = 123$ K a transversal SDW (T-SDW) state (AF_1) is observed with the spins perpendicular to **Q**. Below T_{sf} the spins are parallel to the modulation, which is known as the longitudinal SDW (L-SDW) state (AF_2). Furthermore, a third AF state without a modulation of the spins can be observed in non-single crystal samples and in Cr alloys [8,10]. This AF commensurate state (AF_0) exists up to temperatures above the T_N of single crystalline Cr [8].

It has become an interesting challenge to determine the AF phase diagram of thin Cr films, whether or not they are embedded in a superlattice, and to compare it with the bulk properties. An excellent review of the spin density wave magnetism of thin Cr films was recently published by Zabel [11]. Several papers have already been devoted to the interplay between the structural features and the anti-ferromagnetic phase diagram of thin Cr films. In a study of Sonntag et al. [12] the strain and its non-Poisson behavior in Cr thin films grown on a Nb(110) buffer layer on sapphire substrates has been investigated. Synchroton X-ray studies on such Cr/Nb(110) sapphire films revealed an orientational pinning effect of the SDW-related strain density- and charge density wave [13]. Bödeker et al. [14] reported on the structural and magnetic properties of Cr films, grown on the sapphire/Nb system, and covered with ferromagnetic and paramagnetic layers.

In this paper we aim to add to the body of experimental work by reporting on a detailed study of a 450-nm Cr film of which the structure was thoroughly characterized in order to shed light on the influence of epitaxial strain on the anti-ferromagnetism of Cr. For that purpose, we have prepared by MBE a 450-nm Cr thin films on a MgO(001) single crystal substrate. Our choice of MgO(001) substrates is motivated by the fact that a good epitaxial growth can be achieved [15] and, moreover, because it is frequently used as substrate to grow anti-ferromagnetically coupled Fe/Cr superlattices. Structural information about the sample is obtained from atomic force microscopy (AFM), X-ray diffraction (XRD), and Rutherford backscattering and channeling spectroscopy (RBS/C). In order to study the magnetic behavior, high angle neutron diffraction experiments were carried out at various temperatures. We show that the structural characterization gives evidence for a small epitaxial strain in the films, which leads to a particular orientation of the propagation direction of the SDW and a polarization direction of the Cr spins. Our results are discussed in the light of other studies on the anti-ferromagnetic nature of thin Cr films and are compared to observations of the AF state in strained bulk Cr crystals.

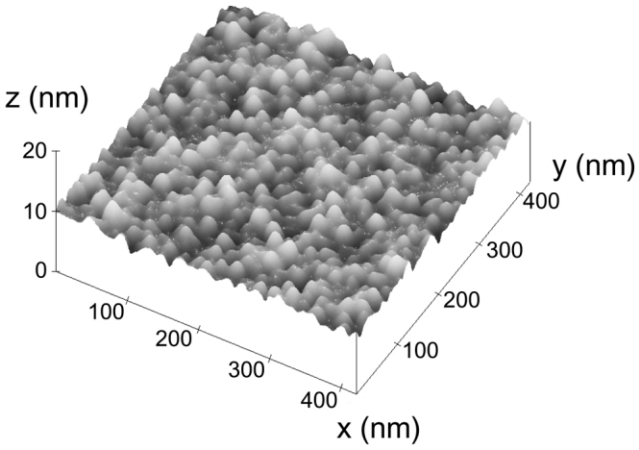

Fig. 1. AFM topography of the surface of the epitaxial Cr film. Analysis of the AFM images yields a root mean square surface roughness of 0.75 nm and an in-plane grain size of the order of 10–20 nm.

2. Preparation and characterization

The Cr film was prepared in a Riber MBE system at a base pressure of 5×10^{-11} mbar which increased to 1×10^{-9} mbar during growth. The 2×2-cm^2 MgO(001) substrate was cleaned by annealing at 600 °C for 15 min in ultra high vacuum. After cooling down, a Cr layer of 4500 Å (99.999% purity) is deposited at a substrate temperature of 100 °C using electron beam evaporation at a rate of 0.4 Å/s. This range of substrate temperature was also used for the preparation of epitaxial Fe/Cr superlattices in which GMR effects were studied [16]. The growth rate is controlled by a quadrupole mass spectrometer system. X-Ray diffraction measurements are performed on a 12-kW Rigaku DMax rotating anode diffractometer using CuK_α (1.54187 Å) radiation and a thin film attachment goniometer with a post-sample crystal monochromator in the Bragg–Brentano configuration.

Fig. 1 shows the topography of the sample surface, measured by atomic force microscopy (AFM). The AFM data were collected on a standard Digital Instruments Nanoscope III instrument, using the Tapping Mode procedure. The sample was at room temperature

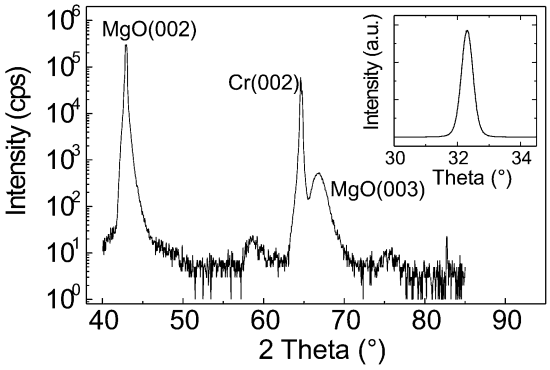

Fig. 2. High angle XRD pattern, revealing only a Cr(002) reflection at $2\theta = 64°$, indicating that the sample is completely (002) oriented. The inset shows the rocking curve around the Cr(002) reflection.

and in ambient conditions for these measurements. The AFM images show a homogeneous and smooth film surface, with a root mean square (r.m.s.) roughness of the order of 0.75 nm, measured over an area of 1×1 μm^2. This is comparable with previous AFM results obtained on epitaxial Cr films on MgO [15]. The same r.m.s. roughness value was found at different positions on the sample surface. Analysis of the AFM images provides furthermore an estimate of the in-plane grain size, which is of the order of 10–20 nm.

High angle XRD measurements on this Cr film are shown in Fig. 2. At $2\theta = 42.95°$ the MgO(002) reflection is observed and a MgO(003) reflection is visible at $2\theta = 66.9°$. The only observed Cr diffraction peak is Cr(002) at $2\theta = 64.62°$ indicating that the sample is completely (002) oriented. The double peak structure in the Cr(002) reflection is caused by the $CuK_{\alpha 1}$ ($\lambda_{\alpha 1} = 1.540598$ Å) and $CuK_{\alpha 2}$ ($\lambda_{\alpha 2} = 1.544418$ Å) contributions to the radiation. The lattice parameter perpendicular to the plane of the sample as determined from these reflections is $d^{\perp} = 2.882 \pm 0.001$ Å, differing little from the bulk value $d^{bulk} = 2.884 \pm 0.001$ Å [17]. The inset of Fig. 2 shows the rocking curve measured around the Cr(002) reflection, which has a full width at half maximum of less than 0.5°, representing a small mozaic spread of the grains. Off-axis XRD measurements around the (112) type reflections allow determination of the epitaxial relation between Cr(001) and the MgO(001) substrate: the cubic bcc Cr unit cell is rotated over 45° with respect to the cubic MgO unit cell, while their [001] axes remain parallel. We denote this epitaxial relationship as MgO(001)[110]//Cr(001)[100].

Fig. 3 shows the Rutherford backscattering (RBS) measurements on this film using a 2.9-MeV He^+ beam, from which a Cr thickness of 4600 Å was determined. In order to probe the crystalline quality of the Cr layer, a channeling measurement with the incoming He beam aligned along the Cr[001]‖MgO[001] axis was performed (Fig. 3a). The backscattering yield in the aligned geometry should be compared to the one for random incidence, which in this case was 8° off-axis from the aligned geometry. This aligned geometry results in a drastic reduction of the backscattering yield, quantified by the minimum yield χ_{min} (which is defined as the ratio of the backscattering yield with aligned and random incidence, respectively). The theoretically expected χ_{min} value for channeling along a Cr[001] axis ranges from 1.7% for a perfect single crystal, to 100% for a polycrystalline structure. From our measurement, shown in Fig. 3a, a χ_{min}-value of ~16% could be deduced, indicating a high defect concentration. Apart from a slight increase at the surface (due to backscattering from the first monolayers), near 2.12 MeV, and the interface, near 1.75 MeV, a relatively constant channeling yield is observed. At the interface, a significant increase of the aligned spectrum indicates enhanced scattering from lattice imperfections, such as misfit dislocations. These misfit dislocations are due to relaxation of the elastically strained Cr layer.

Additional channeling measurements were performed along the off-normal [011] and [111] crystal directions, the latter shown in Fig. 3b. From the positioning of the respective axes in the Cr layer and the MgO substrate, the epitaxial nature of the thin film is confirmed, with its azimuthal orientation being Cr(001)‖MgO(001) and Cr[100]‖MgO[110], i.e. the Cr lattice is azimuthally rotated by 45° with respect to the substrate. The minimum yield measured along the Cr[111] axis is 45%,

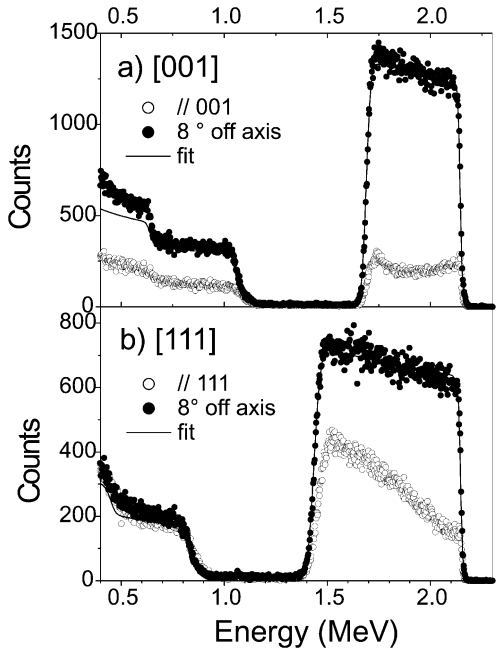

Fig. 3. Rutherford backscattering spectra with random (●) and aligned (○) beam incidence for the Cr[001] (a) and Cr[111] (b) axes. The solid line is a simulation of a 4600-Å Cr film on a MgO substrate using the RUMP-code.

which is much larger than the estimated value of $\chi_{min}=$ 1.5% for a perfect Cr lattice. Moreover, the width of the [111] channeling profile is also much larger than theoretically expected. These observations point to the presence of crystal defects, such as a granular structure and/or mosaicity of the Cr layer.

From the exact position of the Cr channeling minima, the elastic strain of the film can be determined. The angle between the [111] axis and the [001] axis, which is 54.74° in a fully relaxed cubic lattice, will increase (resp. decrease) when a tensile (resp. compressive) strain is applied in the direction parallel to the interface. For a Cr film grown pseudomorphically on a MgO substrate, elasticity theory predicts a tetragonal distortion $\varepsilon^{T}=6.6\%$ (using a Poisson ratio $\nu=0.21$ for Cr), resulting in an increase of 1.77° of the angle $\Delta\psi$ between Cr[001] and Cr[111]. From the measurement of the position of the $[111]_{Cr}$ (at $\sim$54.74°) and the $[32\bar{2}]$, $[75\bar{5}]$ and $[43\bar{3}]$ axes (at $\sim$45°), a very small $\Delta\psi\sim0.09°$ was derived, corresponding to a small $\varepsilon^{T}=0.16\%$. This shows that the Cr layer is nearly completely relaxed but that a minor tensile strain is still present.

3. Neutron diffraction

All neutron diffraction measurements are carried out at the E1 triple-axis spectrometer with polarization analysis of the Berlin Neutron Scattering Center (BENSC) using a wavelength λ of 2.422 Å. The polarization analysis option is not used in these measurements. The sample is mounted in a cryofurnace with a temperature range of 1.5–600 K.

The location of the possible magnetic reflections in the reciprocal space is shown in Fig. 4. The simple antiferromagnetic commensurate state (AF_0) has the period of a single Cr unit cell and can therefore be observed at the (100)-type reciprocal positions. For unpolarized neutron diffraction the magnetic scattering amplitude is proportional to the sine of the angle between the scattering vector $\mathbf{q}$ ($|\mathbf{q}|=4\pi\sin\vartheta/\lambda$) and the direction of the spins [18–20]. This means that the AF_0 structure shown in Fig. 4a with the spins out-of-plane can only be observed at the (100) and (010) reciprocal positions, and not at (001). The reciprocal lattice positions where the out-of-plane AF_0 phase can be observed, are indicated by a thick black dot. In the SDW-phase the magnitude of the spins is sinusoidally modulated. This incommensurate order gives rise to scattered intensity (of magnetic origin) at satellites around the (100)-type reciprocal lattice points. The distance (in reciprocal space) between the satellites and the (100)-type reciprocal lattice points is denoted by δ. The value for δ in units of $2\pi/a$, with a the Cr lattice constant, ranges between 0.048 at low temperature up to 0.036 near the Néel temperature for bulk Cr.

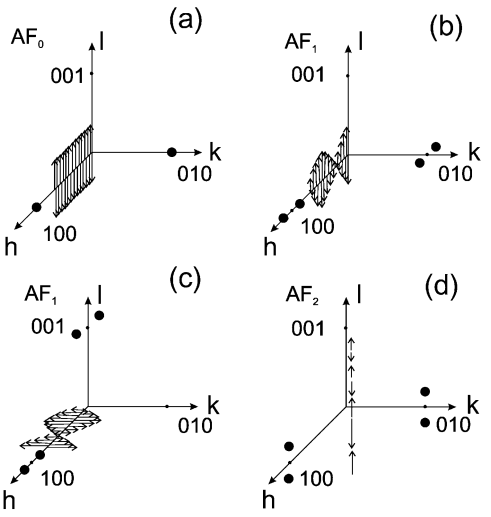

Fig. 4. Overview of the different magnetic states of Cr (spins indicated by arrows) and the corresponding magnetic reflections (indicated by thick black dots) in reciprocal space. The axes are labeled by *h*, *k*, and *l*. The location of the (001) type reciprocal lattice points is indicated by small black dots. (a) Anti-ferromagnetic commensurate state (AF_0) with spins out of plane; (b) transverse spin density wave (AF_1) with spins out-of-plane; (c) transverse spin density wave (AF_1) with spins in-plane; (d) longitudinal spin density wave (AF_2) with spins out of plane.

Fig. 4b gives a schematic presentation of a T-SDW, propagating in-plane and with spins out-of-plane. The thick black dots represent the reciprocal lattice positions of the satellites where scattered intensity from the T-SDW can be observed. Fig. 4c shows a T-SDW, in this case with the spins all in-plane. The thick black dots denote again the reciprocal space positions where scattered intensity from the SDW may be expected. For completeness, Fig. 4d provides a schematic presentation of a L-SDW with the propagation vector out of plane. The black dots represent the reciprocal lattice positions of the observable satellites. It is already worth mentioning that a L-SDW was not observed in these experiments.

In order to investigate the different SDW and their orientations we measured around the $(1\pm\delta,0,0)$ and $(1,0,\pm\delta)$ positions ($\mathbf{Q}$ in-plane), as well as around the $(0,0,1\pm\delta)$ and $(\pm\delta,0,1)$ positions ($\mathbf{Q}$ out-of-plane). Measurements were taken between 20 and 400 K in steps of approximately 50 K. A major experimental problem in neutron diffraction on thin films is the rather small amount of scattering material and, hence, low intensities and relatively long counting times. The alignment of the sample was, therefore, carefully optimized using the single crystalline MgO(001) substrate reflection which produces an intense peak. Due to the epitaxial relationship between MgO and Cr, the Cr reflections are easily found.

Fig. 5 shows the neutron diffraction scans on the Cr film around the $(1\pm\delta,0,0)$ reflections (i.e. along the *h*

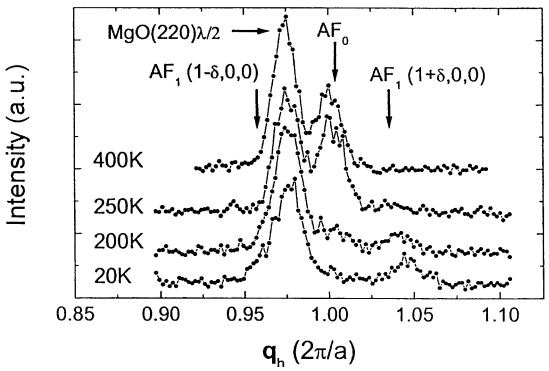

Fig. 5. Neutron diffraction scans along the *h* axis and along the $(1\pm\delta,0,0)$ satellite reflections. The most prominent peak is caused by the MgO(220) substrate reflection. Between 200 K and 250 K a transition occurs from a transversal spin density wave (indicated by the AF_1 satellite reflections) towards the commensurate anti-ferromagnetic phase (indicated by AF_0). For clarity, the curves have been shifted vertically.

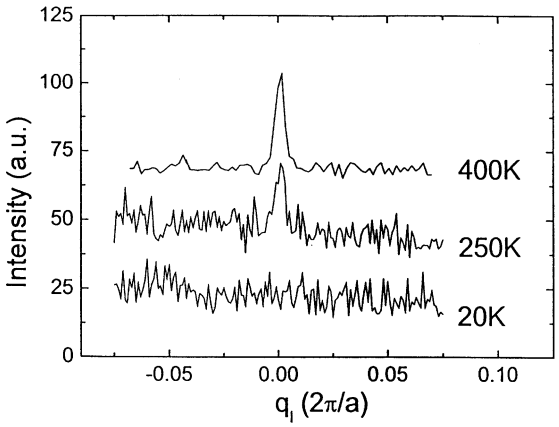

Fig. 6. Neutron diffraction scans parallel to the *l* axis and along the $(1,0,\pm\delta)$ satellites. At low temperatures, no satellite peaks can be observed at the $(1,0,\pm\delta)$ positions, indicating the absence of a L-SDW with propagation vector out of plane. At higher temperatures a peak can be observed at the (1,0,0) position, confirming the presence of an AF_0 phase with spins pointing out of plane.

axis) as function of temperature. The reflection at $\mathbf{q_h} = 0.975$ Å^{-1} is due to the incompletely filtered out neutrons with wavelength $\lambda/2$ diffracted from the MgO(220) planes. At 20 K the $(1+\delta,0,0)$ satellite reflection can be observed at $\mathbf{q_h} = 1.045$ Å^{-1} proving the presence of a T-SDW with in-plane propagation direction. The other satellite, $(1-\delta,0,0)$, is for the greater part covered by the MgO(220) peak. The polarization of this in-plane T-SDW can be derived from the measurements around the $(\pm\delta,0,1)$ positions. We did not find any indication for an in-plane direction of the spins and therefore we assume that the spins are polarized perpendicular to the plane of the film. Due to experimental difficulties (tilting of the cryofurnace) it was not possible to confirm this by measurements around the $(\pm\delta,1,0)$ positions. At 200 K the $(1+\delta,0,0)$ reflection decreases and a small intensity increase at the (1,0,0) position can be observed. At 250 K a clear peak shows up at (1,0,0) indicating the presence of a simple anti-ferromagnetic commensurate state while the T-SDW disappears. We could not observe any change in intensity at the (001) position during this transition, hence we conclude that the spins in the AF_0 state point out-of-plane. This state remains present up to the highest measured temperature of 400 K which is above the Néel temperature of single crystalline Cr.

Fig. 6 shows the neutron diffraction results for a scan along the $(1,0,\pm\delta)$ satellites, i.e. parallel to the *l* axis. The absence of any clear satellites indicates that there is no L-SDW with propagation vector out of plane. At 400 K we observe a peak at the (1,0,0) position, confirming the presence of an AF_0 phase with the spins pointing out of plane.

An overview of the intensity of the AF_0 and AF_1 state for all measured temperatures is given in Fig. 7, in which the normalized integrated intensities of the AF_0 and AF_1 reflections are plotted vs. temperature. The transition from an in-plane T-SDW towards the simple commensurate phase occurs between 200 and 250 K. We did not observe any indication for a L-SDW over the whole temperature range.

The tetragonal distortion measured by XRD and RBS has also been observed by neutron diffraction. Using $\lambda/2$ neutrons we measured the out-of-plane nuclear Cr(002) reflection. The position of the magnetic in-plane Cr(100) reflection, due to the AF_0 state, differs by $0.3\pm0.07°$ from the above mentioned nuclear Cr(002) reflection. Based on these results we find for the out-of-plane Cr(001) lattice parameter $d^{\perp} = 2.882\pm0.001$ Å and for the in-plane Cr(100) lattice parameter $d^{\parallel} = 2.895\pm0.005$ Å, which gives a $\Delta\psi = 0.12\pm0.06°$ (angle between Cr[111] and Cr[001]),

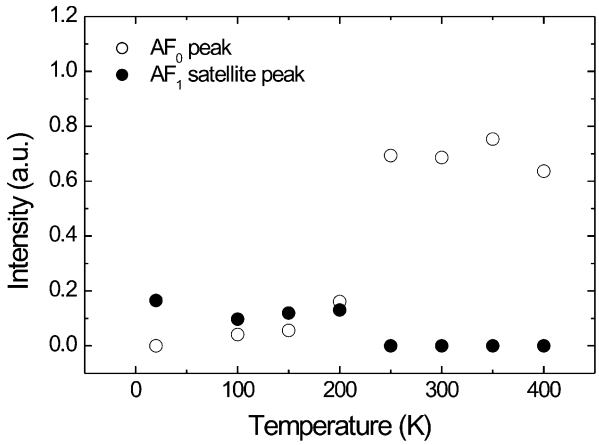

Fig. 7. Evolution of the integrated and normalized intensity of the Cr(100) AF_0 (○) and the Cr$(1+\delta,0,0)$ AF_1 (●) reflection as a function of temperature.

which is, within the error, in agreement with the RBS observations.

4. Discussion

For the discussion of these results, it is instructive to compare with the experimental and theoretical results that were obtained on bulk single crystalline samples, as well as with the more recently published studies on thin Cr films.

Two main differences become clear when we compare the magnetic state of bulk single crystalline Cr with the one observed in our epitaxial Cr thin film on MgO. The first is the different temperature dependence of the magnetic phase diagram and the observation of the AF_0 state in the film. The second is the clear preferential **Q**- and spin direction observed in the Cr film, an anisotropy which is absent in bulk single crystal Cr.

The commensurate AF_0 state has been observed in bulk Cr by neutron diffraction and has led to confusion about the T_N of Cr [8,21]. Bacon et al. [22,23] related the presence of the commensurate state in pure Cr to the disruption of the periodic lattice due to defects and their strains. Loss of the periodicity seems to be essential since this state has not been observed in Cr single crystals [24]. This is qualitatively in agreement with the calculations of Rice [25], who studied the effect of an imperfect nesting of the Fermi and hole surfaces and found a first order behavior of the **Q** vector for the commensurate–incommensurate transition. The itinerant anti-ferromagnetism in Cr is explained as originating from this nesting of the Fermi surface [8,26,27]. Loss of the periodicity due to defects and their strains could influence the band bending near the Bragg planes and thus alter this surface. Based on the high backscattering yield in the RBS/C experiments we conclude that disruption of the lattice periodicity due to defects and their strains is the reason for the observation of the AF_0 state in our epitaxial Cr film. In addition we did not observe a continuous change in the **Q** vector confirming the first order nature of the AF_1–AF_0 transition.

The observed temperature dependence of the magnetic phase diagram (shown in Fig. 7) is in agreement with the observations of Bacon [22] and Window [28]. Apart from the presence of the AF_0 state, a broadening of the transition temperatures (T_N and T_{sf}) was found with a suppression of the AF_2 state. In our measurements the AF_2 state could not be observed within the resolution of the experiment.

Williams and Street [29,30] proposed a model for calculating the magnetic phase diagram in strained Cr and found a reasonable agreement with the experimental observations. Our experimental observations display a much stronger temperature dependence of the AF_0 state than their model predicts. In principle, this discrepancy could be explained by assuming a higher defect concentration. This would imply, however, a stronger presence of the AF_0 state at low temperatures. This is not observed in our experiments, where the AF_0 state can be observed to vanish rather abruptly below 200 K.

The orientation of the spins can be influenced by the application of strain. Bastow et al. [31] showed that cooling through the Néel temperature while applying compressive stress produces samples with the **Q** vectors perpendicular to the stress direction. These observations are confirmed by the theoretical calculations of the effect of compressive stress along a crystal axis by Barak et al. [32], who found that the most stable direction for **Q** vectors is the one perpendicular to which the compressive stress is applied. Furthermore, they derived that the polarization of the spins will be parallel to the axis along which the compressive strain is applied. In our sample a small stress is induced by a 3% difference in lattice parameter between the MgO substrate and the Cr film. Adaptation of the Cr unit cell to the MgO unit cell will result in an expansion of the Cr in-plane lattice parameter and shrinking of the out-of-plane Cr lattice parameter as observed from the XRD, RBS and neutron diffraction results. Taking the experimentally obtained values for $d^{\perp}$ and $d^{\parallel}$ and using the values of single crystal Cr for the elastic constants $C_{11} = 3.398 \times 10^{11}$ N/m^2 and $C_{12} = 0.586 \times 10^{11}$ N/m^2 [33], one can derive that a compression pressure of the order of 10^7 N/m^2 is needed for such a deformation. This value is in agreement with the compressive cooling experiment of Bastow et al. where a compression pressure of 7×10^6 N/m^2 was used. However, it is necessary to mention that the values for the lattice parameters are averaged over the whole thickness of the sample. From the RBS measurements it is clear that in the first grown layers (Fig. 3a, near 1.7–1.8 MeV) a relaxation occurs and therefore a higher distortion could be present in this region.

It is very instructive to compare the results on our Cr film with the results that were obtained by several other groups and which were recently reviewed by Zabel [11]. Several experiments have been reported on the proximity effects between a ferromagnetic layer and the antiferromagnetic Cr layer [4,6,7,34–36], but here we will focus on the experimental results obtained on Cr films in contact with paramagnetic substances. It was established by neutron diffraction and perturbed angular correlation spectroscopy (PAC) that a 250-nm Cr film grown on the Nb/Al_2O_3 system predominantly shows a longitudinal SDW with propagation vector out of plane [37]. At higher temperatures an AF_0 state with the spins out of plane was observed. These results are very important because it was one of the few studies where a cross-correlation was made between the neutron diffraction results and those from an entirely different technique (PAC). Somewhat thicker Cr films (300–400

nm) grown on the Nb/Al_2O_3 system also exhibited a predominant longitudinal SDW state with the spins out of plane [38]. Bödeker et al. [14] studied the influence of non-magnetic overlayers by capping 200-nm Cr films with 2-nm Cu or 3-nm Pd layers. The Cu-covered films again displayed the L-SDW with **Q** out of plane. For the Pd-covered Cr films, contributions were observed from a L-SDW with **Q** out of plane as well as from a T-SDW with **Q** in plane. Sonntag et al. also studied 200–300-nm-thick Cr films on MgO substrates and observed a SDW with wavevectors in all possible {001} directions, comparable to the observations in unstrained single crystalline bulk Cr [39]. Finally, the magnetic ordering in Cr layers embedded in a Cr/Ag superlattice was also studied by the PAC method [40]. For Cr layers with a thickness varying from 3 to 8 nm, a L-SDW with **Q** normal to the layers was observed, from the lowest temperatures all the way up to 500 K. The general trend which emerged from these experiments is, therefore, that the L-SDW phase is predominant and that, contrary to the expectations, the propagation vector does not coincide with the plane in which the tensile strain is present.

The neutron diffraction results presented in this paper differ on a number of points with the experiments cited above. First of all, at low temperatures a predominant T-SDW was observed, while no indications could be found for the existence of a L-SDW phase. Secondly, the propagation vector for the T-SDW is in the plane of the Cr film, which does coincide with the direction of the tensile strain, as was determined from the structural analysis. At higher temperatures a commensurate AF_0 phase with the spins perpendicular to the film plane was observed. We believe that the epitaxially induced strain could be the reason for the presence of only in-plane propagating T-SDW with the Cr spins along the out-of-plane [001] direction. The difference with previously reported results may be caused by a somewhat more dominating effect of the strain or by the absence of additional electronic effects which may play a role, e.g. at the interface between Cr and the Nb buffer layer. Comparing these results with previously available data underlines once more that subtle differences in the structure of the layers may lead to significant variations in the magnetic ordering of the Cr layer.

5. Conclusions

We have reported on an epitaxial Cr(001) film with thickness of 450 nm, grown on MgO, which was characterized in detail using AFM, RBS, and XRD. The magnetic phase diagram for this epitaxial Cr film was established using neutron diffraction and is in agreement with the observations for bulk strained polycrystalline Cr. Below 200 K an incommensurate transversal spin density wave is found with a propagation vector in the film plane, i.e. coinciding with the plane of tensile strain. Between 200 and 250 K there is a transition from the incommensurate T-SDW towards a commensurate AF_0 state in which the spins are pointing out of plane. The small mismatch between the MgO substrate and the Cr film is believed to produce an epitaxial stress causing the spins of the Cr to align along the [001] direction and the **Q** vector along the tensile stress direction. Comparing these results with previously reported data on the magnetic ordering in epitaxial Cr films stresses once more that small differences in the structural parameters of the films leads to significant differences in the magnetic phase diagram.

Acknowledgments

We thank M.J. Van Bael and J. Swerts for valuable contributions. This work is supported by the Fund for Scientific Research-Flanders (FWO), the Belgian Interuniversity Attraction Poles (IUAP) and the Flemish Geconcerteerde Onderzoeksacties (GOA) Programs, and the European Commission, in the framework of the TMR Program, LSF contract ERBFMGE CT950060. E.K. is supported by the Flemish institute for the promotion of research in industry (IWT). K.T. is a postdoctoral research fellow of the FWO. S.M. was financed by the Copernicus program of the European Commission, contract ERB-IC15-CT96-0751.

References

[1] D.E. Bürgler, P. Grünberg, S.O. Demokritov, M.T. Johnson, in: K.H.J. Buschow (Ed.), Handbook of Magnetic Materials, vol. 13, Elsevier, Amsterdam, 2001, p. 1.
[2] E.E. Fullerton, D.M. Kelly, J. Guimpel, I.K. Schuller, Y. Bruynseraede, Phys. Rev. Lett. 68 (1992) 859.
[3] R. Schad, P. Beliën, G. Verbanck, V.V. Moshchalkov, Y. Bruynseraede, H.E. Fischer, S. Lefebvre, M. Bessiere, Phys. Rev. B 59 (1999) 1242.
[4] J. Meersschaut, J. Dekoster, R. Schad, P. Beliën, M. Rots, Phys. Rev. Lett. 75 (1995) 1638.
[5] E. Fullerton, K.T. Riggs, C.H. Sowers, S.D. Bader, A. Berger, Phys. Rev. Lett. 75 (1995) 330.
[6] E. Fullerton, S.D. Bader, J.L. Robertson, Phys. Rev. Lett. 77 (1996) 1382.
[7] A. Schreyer, C.F. Majkrzak, Th. Zeidler, T. Schmitte, P. Bödeker, K. Theis-Bröhl, A. Abromeit, J.A. Dura, T. Watanabe, Phys. Rev. Lett. 79 (1997) 4914.
[8] E. Fawcett, Rev. Mod. Phys. 60 (1988) 209.
[9] S.A. Werner, A. Arrott, Phys. Rev. 155 (1967) 528.
[10] E. Fawcett, H.L. Alberts, V.Yu. Galkin, D.R. Noakes, J.V. Yakhmi, Rev. Mod. Phys. 66 (1994) 25.
[11] H. Zabel, J. Phys.: Condens. Matter 11 (1999) 9303.
[12] P. Sonntag, W. Donner, N. Metoki, H. Zabel, Phys. Rev. B 49 (1994) 2869.
[13] P. Sonntag, P. Bödeker, T. Thurston, H. Zabel, Phys. Rev. B 52 (1995) 7363.
[14] P. Bödeker, A. Schreyer, H. Zabel, Phys. Rev. B 59 (1999) 9408.

[15] R. Schad, P. Beliën, G. Verbanck, C.D. Potter, K. Temst, V.V. Moshchalkov, Y. Bruynseraede, J. Magn. Magn. Mater. 182 (1998) 65.
[16] P. Beliën, R. Schad, C.D. Potter, G. Verbanck, V.V. Moshchalkov, Y. Bruynseraede, Phys. Rev. B 50 (1994) 9957.
[17] W.B. Pearson, Handbook of Lattice Spacings and Structures of Metals, vol. 2, Pergamon Press, Oxford, 1967, p. 819.
[18] O. Halpern, M.H. Johnson, Phys. Rev. 55 (1939) 898.
[19] G.E. Bacon, Neutron Diffraction, Clarendon Press, Oxford, 1975.
[20] D.E.G. Williams, The Magnetic Properties of Matter, Longmans, London, 1966.
[21] C.G. Shull, M.K. Wilkinson, Rev. Mod. Phys 25 (1953) 100.
[22] G.E. Bacon, Acta Cryst. 14 (1961) 823.
[23] G.E. Bacon, N. Cowlam, J. Phys. C 2 (1969) 238.
[24] T.M. Sabine, G.W. Cox, J. Phys. Chem. Solids 27 (1966) 1955.
[25] T.M. Rice, Phys. Rev. B 2 (1970) 3619.
[26] W.M. Lomer, Proc. Phys. Soc. (Lond.) 80 (1962) 489.
[27] J.B. Staunton, J. Poulter, B. Ginatempo, E. Bruno, D.D. Johnson, Phys. Rev. Lett. 82 (1999) 3340.
[28] B. Window, J. Phys. C 2 (Suppl.) (1970) S210.
[29] I.S. Williams, E.S. Raja Copal, R. Street, J. Phys. F 9 (1979) 431.
[30] I.S. Williams, R. Street, Philos. Mag. B 43 (1981) 893.
[31] T.J. Bastow, R. Street, Phys. Rev. 141 (1966) 510.
[32] Z. Barak, Q.B. Walker, J. Phys. F 12 (1982) 483.
[33] D.R. Lide, Handbook of Chemistry and Physics, 79th ed., 1998–1999, CRC Press, London, 1998.
[34] P. Bödeker, A. Hucht, A. Schreyer, J. Borchers, F. Güthoff, H. Zabel, Phys. Rev. Lett. 81 (1998) 914.
[35] P. Bödeker, P. Sonntag, A. Schreyer, H. Zabel, J. Borchers, K. Hamacher, H. Kaiser, J. Appl. Phys. 81 (1997) 5247.
[36] H. Fritzsche, J. Hauschild, A. Hoser, S. Bonn, J. Klenke, Europhys. Lett. 49 (2000) 507.
[37] J. Meersschaut, J. Dekoster, S. Demuynck, S. Cottenier, B. Swinnen, M. Rots, Phys. Rev. B 57 (1998) R5575.
[38] P. Sonntag, P. Bödeker, A. Schreyer, H. Zabel, K. Hamacher, H. Kaiser, J. Magn. Magn. Mater. 183 (1998) 5.
[39] P. Sonntag, Magnetic and Structural Properties of Thin Epitaxial Cr Films, Ph.D. Thesis, Ruhr-Universität Bochum, Germany, 1996.
[40] S. Demuynck, J. Meersschaut, J. Dekoster, B. Swinnen, R. Moons, A. Vantomme, S. Cottenier, M. Rots, Phys. Rev. Lett. 81 (1998) 2562.